



Quantitative relationship between weather seasonality and rock fall occurrences north of Hope, BC, Canada

Christopher Pratt¹ · Renato Macciotta²  · Michael Hendry³

Received: 4 April 2018 / Accepted: 26 July 2018 / Published online: 7 August 2018
© Springer-Verlag GmbH Germany, part of Springer Nature 2018

Abstract

The relationship between rock falls and weather conditions has been widely recognized and attempts have been made to develop weather-based approaches for rock fall hazard management. This dependency of rock fall occurrences on weather suggests that rock fall trends and their associated risks will vary following climatic changes. In this regard, tools that quantify the relationship of weather seasonality and climate with rock fall trends provide an opportunity to forward model potential variations in rock fall trends considering diverse climate scenarios. This paper illustrates the application of one such tool along a section of a transportation corridor through the Canadian Cordillera. von Mises probability distributions are fitted to monthly trends of precipitation and freeze–thaw cycles and combined to develop a probability density model of rock fall occurrences. The methodology is outlined in detail and the model shown to fit the rock fall database with a correlation coefficient of 0.97. Further, the paper discusses limitations of the approach and potential opportunities for improvement, encouraging the use of the method at other sites and building a robust case study database for further enhancement of the approach.

Keywords Rock falls · Weather seasonality · Triggers · von Mises distribution

Introduction

The negative impacts of rock fall occurrences on transportation corridors through the Canadian Cordillera have been widely recognized (Bunce et al. 1997; Evans and Hungr 1993; Hungr et al. 1999; Lan et al. 2010; Macciotta et al. 2011, 2013;

Peckover and Kerr 1977; Piteau 1977). This has led to resource allocation for rock fall hazard control in terms of protection, stabilization, monitoring, and research and development of enhanced risk mitigation strategies (Kromer et al. 2015; Lato et al. 2012; Macciotta and Martin 2013; Macciotta et al. 2015a, 2016, 2017a; Rodriguez et al. 2017; van Veen et al. 2017). Part of this effort has focused on improved correlations between weather seasonality or weather events and rock fall occurrences, with the aim of providing predictive analysis for periods of higher rock fall hazard (Macciotta et al. 2013, 2015b) or potential rock fall trend changes with future climate change (Macciotta and Hendry 2017; Macciotta et al. 2017b). Rock fall processes are initiated by block detachment from a slope by sliding (planar or wedge), toppling, or purely tensile fracture from overhangs, all of which are known to be potentially triggered by increased water pressures (Higgins and Andrew 2012). Further, intact rock degradation has also been reported following freeze–thaw cycles (Yavuz 2010), which can lead to cohesion loss and block detachment. The causality between rock fall occurrences and weather has also been well established and recognized in many studies around the world based on observations of rock fall/ weather records. These include those studies by Luckman (1976), Douglas (1980), Pierson et al. (1990), Wiczorek and Jäger (1996), Frayssines and Hantz (2006), Higgins and

✉ Renato Macciotta
macciott@ualberta.ca

Christopher Pratt
cspratt@ualberta.ca

Michael Hendry
hendry@ualberta.ca

¹ Department of Civil and Environmental Engineering, Donadeo Innovation Centre for Engineering, University of Alberta, Edmonton, Alberta T6G 1H9, Canada

² David and Joan Lynch School of Engineering Safety and Risk Management, 12-324 Donadeo Innovation Centre for Engineering, University of Alberta, Edmonton, Alberta T6G 1H9, Canada

³ Department of Civil and Environmental Engineering, 6-263 Donadeo Innovation Centre for Engineering, University of Alberta, Edmonton, Alberta T6G 1H9, Canada

Andrew (2012), and Delonca et al. (2014). This causality has also been established for areas in southwest British Columbia by Piteau (1977) and Macciotta et al. (2015b).

Changes in climate and weather trends would modify the magnitude, intensity, and frequency of climatic events that can cause landslides (Coe 2017) and the precursory factors for landslide events (antecedent precipitation, freeze–thaws, etc.) (Ho et al. 2017). This can be intensified particularly for shallow landslides, including rock falls. In the southwestern area of the Canadian Cordillera, where the higher density of transportation corridors is located, precipitation is projected to decrease in the summer and fall (Bush 2015; Bush et al. 2014) and timing for freeze–thaw cycles to concentrate on the winter months and decrease during the fall and spring (Logan et al. 2011). This would lead to changes in the timing, frequency, and size of landslide occurrences (Cloutier et al. 2017), particularly rock falls. Some researchers have studied the correlations between rock fall occurrences and weather events and the potential influences of changing climate (Delonca et al. 2014; Raveland and Deline 2011, 2015; Paranunzio et al. 2015, 2016). These studies were mostly on European countries and focused on the occurrence of specific events. Some of them also focused on particular sets of weather conditions leading to the rock fall events. However, there is a gap in studies attempting a quantitative correlation between weather trends and rock fall occurrences in the Canadian Cordillera that would allow assessing the impact of changes in weather patterns in rock fall trends. In this regard, Macciotta et al. (2017b) present a methodology for quantifying the relationship between annual rock fall distributions and the seasonal variation of common rock fall triggers across the Canadian Cordillera. The methodology relies on fitting statistical models to these weather triggers (e.g., precipitation, freeze–thaw cycles) and combining them to produce a strong model that fits the rock fall distribution. They illustrate the applicability of the models through one case study. The objective of the present paper is to: (1) further validate the applicability of this methodology through a second case study in the Canadian Cordillera; (2) discuss some of the limitations of the methodology and opportunities for improvement; and (3) provide some standardization for its application such that future studies can be aggregated for further analysis of trends.

General methodology

The methodology proposed by Macciotta et al. (2017b) will be illustrated in detail through a case study in subsequent sections. A summary of the general steps required to apply the method is presented below to provide the reader with a road map for its application:

1. Review rock fall occurrence history with respect to weather conditions (temperature, precipitation, wind speed, etc.) to determine the likely dominant rock fall trigger mechanisms. Previous studies already recognize the dominant trigger mechanisms common to some areas.
2. Calculate average monthly rock fall occurrences and average values for the dominant weather triggers. Ideally, the rock fall database and weather information provide several common years of consistent recording standards. In this regard, the consistency of rock fall recording standards and the completeness of weather data need to be assessed. If these databases are consistent and common through several decades, consideration should be given to climate oscillations that might permit splitting of the data into different time periods.
3. Normalize the monthly rock fall and weather data (triggers) to the average annual totals to provide monthly relative frequencies.
4. Fit probability density functions to the normalized weather triggers. The methodology considers the use of statistics for directional data, fitting the seasonal variation of weather triggers to circular probability density functions.
5. Combine the fitted weather distributions and calibrate against rock fall records. This will provide quantitative relationships between weather patterns and rock fall activity.

The following sections illustrate these steps for a case study in the Canadian Cordillera. The steps are detailed and some standardization for the use of the method is presented.

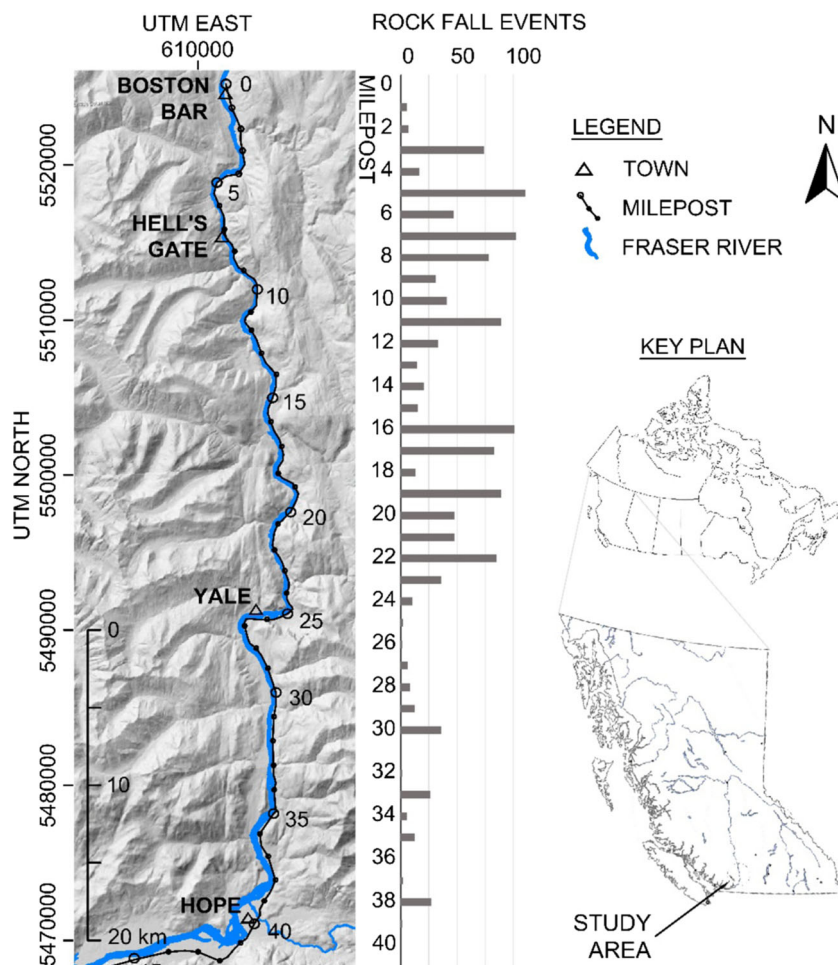
Study area

Location and geologic context

The study area corresponds to part of a railway corridor through the Canadian Cordillera operated by Canadian National Railway (CN) known as the Yale subdivision, which begins near Boston Bar and continues south along the east bank of the Fraser River, terminating in Vancouver, British Columbia (Fig. 1). The alignment of CN's railway tracks between Boston Bar and Hope approximately corresponds to mileposts 0 to 40 of the Yale subdivision on a shaded topographic relief of the area (after Macciotta et al. 2011). The railway alignment is located along the east bank of the Fraser River Valley, alongside steep valley walls and slope cuts. Figure 1 further shows the rock fall distribution per milepost to illustrate its spatial distribution, which is discussed later in this section.

The Fraser River marks the physiographic boundary between the Coast and Cascade mountains (Monger 1970). The area contains various rock types due to a complex geologic history including several episodes of orogenic deformation and intrusion (McTaggart and Thompson 1967). The area

Fig. 1 The Canadian National Railway's (CN) Yale subdivision study area and spatial distribution of rock falls between 1996 and 2016



also features a north–south oriented fault zone known as the Fraser River fault zone. Two major faults are located within the valley: the Hope Fault on the west side of the Fraser River and the Yale Fault, located east of the Hope Fault (Fig. 2). The presence of these faults results in a zone of highly foliated metamorphosed rock with high levels of shearing between rock units and near faults (McTaggart and Thompson 1967).

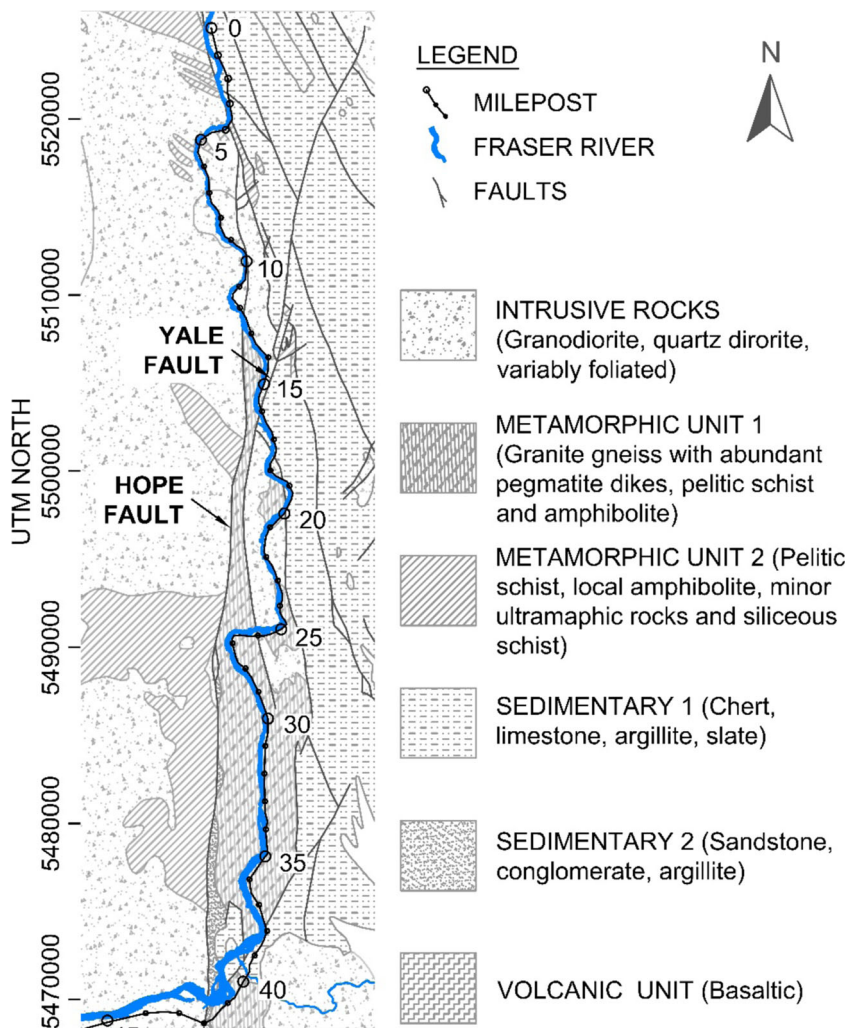
Figure 2 also shows the lithologic units along mileposts 0 to 40 of CN's Yale subdivision and a legend with a description of each unit (after Macciotta et al. 2011). Mileposts 0 to 3 correspond mainly to sedimentary formations, mileposts 4 to 15 to intrusive formations, and mileposts 16 to 23 to intrusive, metamorphic, and sedimentary formations. The remaining section of the line from mileposts 24 to 40 consists of mainly metamorphic formations.

The narrow Fraser Valley was carved by glaciation and subsequent erosion by the Fraser River (Monger 1970) and features many steep, rocky sections along the river, particularly between Boston Bar and Yale. These steep sections, further requiring steep cuts to accommodate the railway alignment, have increased the susceptibility to rock falls. This is evidenced by the concentration of rock fall records between Boston Bar and Yale (Fig. 1).

Rock fall database

The rock fall database consists of CN's rock fall records along the Yale subdivision dating back to 1996. The database is populated mainly by naturally occurring rock falls; however, slope management activities such as scaling and rock bolting influence the rock fall likelihood in these areas. Rock fall events are recorded by rail maintenance crews and train conductors when fallen blocks are observed. Rock fall events include rocks observed on the tracks, rocks observed near the tracks, and evidence of rock fall events that do not specifically affect the tracks. Therefore, the phenomenon analyzed is the result of natural rock detachment mechanisms, their trajectory, and biases introduced by both slope maintenance activities and reporting standards. The rock fall database includes information related to the date, location, and size classification of the event. Rock fall sizes recorded varied from large, infrequent events up to a few thousand cubic meters, down to small blocks of 15 to 30 cm in equivalent diameter. The smaller blocks are only recorded when they are noticeable to crews (on or immediately adjacent to the tracks). The resulting record comprises a subset of rock fall events that have posed a hazard to the

Fig. 2 Geology of the study area (after Macciotta et al. 2011)



railway operation. Secondary information such as if the event blocked the tracks, caused delays, or caused track damage is also included in the database.

A total of 1367 individual rock fall events were recorded between 1996 and 2016, the vast majority (1351) of which occurred between mileposts 1 and 40. Rock fall events occur at greater frequency for certain sections along the subdivision (Fig. 3). Approximately 87% of all rock falls occur between mileposts 3 and 23, with the increased likelihood of rock falls in this area tied to geologic conditions and topography of the track side slopes, which are characterized by steeper cuts in sheared materials.

Figure 4 shows the annual number of rock fall events between mileposts 0 and 40. A discrepancy in frequency is observed between the first two years of records (318 and 484 rock falls per year) and the remaining years (between 2 and 68). A similar change in the frequency of rock fall records is observed for 2012–2016 compared to prior years. Weather patterns have not been observed to drastically change to justify such a discrepancy, with temperatures following consistent annual trends and total precipitation well

within the expected ranges (between 1300 and 2000 mm at Hope). Discussions with CN personnel revealed a change in record standards in 1997 and early 2012, which, unfortunately, is not documented in detail. Therefore, the present study uses rock fall records from 1998 and 2011 to minimize the bias introduced in the analyses.

Section and period for detailed analysis

The section for further detailed analysis was defined based on maintaining a consistent lithology. This minimizes potential biases associated with rock fall sources with diverse

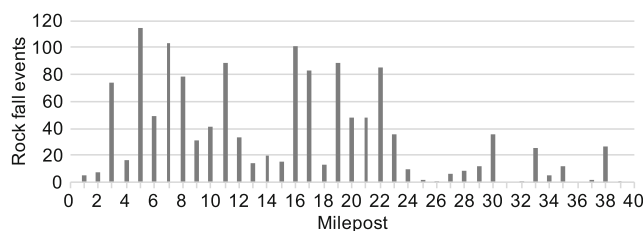


Fig. 3 Recorded rock fall events per milepost between 1996 and 2016

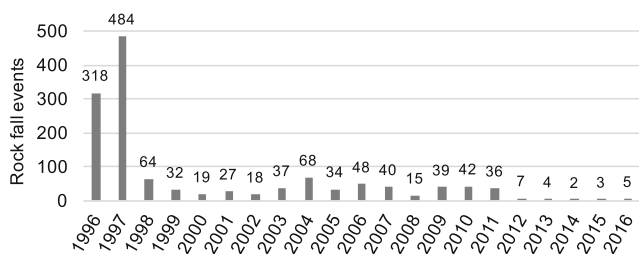


Fig. 4 Recorded rock fall events per year between mileposts 0 and 40

lithology that show different responses to rock fall triggers. The section corresponds to mileposts 4 to 15 of CN's Yale subdivision, which lies mainly on intrusive rocks. The period of analysis corresponds to those years for which the authors consider rock fall recording standards to have been consistent. This corresponds to 14 years of records (1998 through 2011, inclusive), during which 220 rock falls were recorded between mileposts 4 and 15.

Analysis of weather and climate at the study area

Weather data and general trends

Historic weather data were obtained from the Government of Canada's publicly available Historic Climate Database (Environment Canada 2017). Daily total precipitation and daily maximum/minimum temperatures were analyzed to gain an understanding of temporal variations throughout the year. A limitation of this weather database is that the analysis of daily minimum and maximum temperatures would not capture all freeze–thaw events, as this process could occur multiple times a day. Furthermore, elevation changes, incidence of sunlight, shadow effects, etc. will cause temperature variations throughout the study area when compared to the locations of weather stations. In this regard, the maximum and minimum temperatures oscillating around water freezing temperature provide an approximation for the periods of time when freeze–thaw cycles are more frequent and may play a role as rock fall trigger. Therefore, the use of the maximum and minimum temperatures for better understanding the frequency of freeze–thaw cycles and their correlation with rock fall events was considered adequate in light of the information available and for assessing seasonal trends.

Within the study area, weather data were available from weather stations in the towns of Hope, Yale, Hell's Gate, and Boston Bar for the periods shown in Table 1. The only station with continuous records coinciding with the rock fall period (1998–2011) was Hope. Weather data were not evaluated beyond 2011 (the end of the rock fall period considered). Percent completeness (ranging from 97.1 to

99.1%) was evaluated by determining the number of days that were missing inputs for either maximum temperature, minimum temperature, or total precipitation.

Figure 5 presents the seasonal weather data at each station, organized from north to south. The data presented in the figure correspond to the respective data ranges in Table 1. The average daily maximum and minimum temperatures were taken directly from the weather database and plotted as dashed lines. Figure 5 also shows average daily precipitation, calculated as the total monthly precipitation divided by the number of days in the month. Precipitation data are presented as total precipitation, without specifying whether it is rain or snow. Only a portion of the available data included information on the level of snowfall. An evaluation of the data that did include snowfall measurements found that only 6.6% of the total precipitation was recorded as snow.

The average number of monthly freeze–thaw cycles are plotted on the same axis as daily precipitation in Fig. 5. Freeze–thaw cycles were estimated using daily maximum and minimum temperatures. The structure of the database did not allow for consideration of the time above or below freezing or the possibility of multiple cycles per day. A freeze–thaw cycle was considered to have occurred if the daily minimum and maximum temperatures recorded were below $-1\text{ }^{\circ}\text{C}$ and above $+1\text{ }^{\circ}\text{C}$, respectively. The threshold of $-1/+1\text{ }^{\circ}\text{C}$ was chosen to eliminate days in which the temperature was very close to freezing ($0\text{ }^{\circ}\text{C}$) but would likely not cause freezing of liquid water within rock joints. This approach is consistent with previous studies on rock fall trigger mechanisms (Macciotta et al. 2015b, 2017b).

The average daily temperatures generally follow similar trends from the south end of the study area (Hope) to the north (Boston Bar). Temperatures peak in August at all stations, with average daily maximums ranging from $25\text{ }^{\circ}\text{C}$ at Hope to $29\text{ }^{\circ}\text{C}$ at Boston Bar. At Hope and Yale, the lowest average daily temperatures occur in January, while at Hell's Gate and Boston Bar, the lowest temperatures occur in December.

The change in weather trends between the south and north ends of the study area can be attributed to a number of factors. Hope is the furthest south and has a relatively unobstructed path to the Pacific Ocean, resulting in the mildest temperature fluctuations and the highest level of precipitation. Further north in the Fraser River Valley, precipitation decreases and daily/seasonal temperature fluctuations become greater. Table 2 shows the average annual precipitation and number of freeze–thaw cycles at the four weather stations for the periods of available data.

Although the periods of available data differ for the four weather stations, Table 2 clearly shows that Hope has the highest overall amount of precipitation (1847 mm/year). Consistent decreases in precipitation are noted for stations

Table 1 Weather stations along the study area including weather data range and percentage of complete data

Station	Milepost	UTM zone 10		Elevation (m)	Weather data range (years)	Percent complete
		East	North			
Boston Bar	3.5	612586	5524983	200	1980–1989	98.5%
Hell's Gate	8.5	611580	5515694	122	1980–1986	97.1%
Yale	27	613282	5491632	76	1985–1994	99.1%
Hope	40	610114	5469324	39	1980–2011	97.8%

located further north in the valley, with average precipitation at Yale, Hell's Gate, and Boston Bar of 1540, 1211, and 850 mm/year, respectively. Seasonal trends in weather are similar, with peak levels of precipitation occurring in November. All weather stations have a secondary precipitation peak, which occurs in January at Hope and Yale, and February at Hell's Gate and Boston Bar.

The most significant differences in weather data are with respect to the temporal distributions and total number of freeze–thaw cycles. Generally, the average number of freeze–thaw cycles increases from south to north in the valley. In Hope and Yale, freeze–thaw cycles peak in December, then hold roughly steady and drop off after February. At Hell's Gate and Boston Bar, freeze–thaw cycles increase in January, with peaks in February and March.

Correlation of weather trends at Hope to other locations along the study area

Historic weather records were not available at the stations north of Hope for the period of analysis considered for the rock fall data (1998–2011). This is problematic because the majority of rock falls occur approximately 20 to 50 km north of Hope. The similarity of weather trends between stations must be examined to determine the utility of Hope weather data for evaluating rock fall trends further up the valley. Figure 6 presents plots of average monthly precipitation normalized to average annual precipitation (left) and average number of freeze–thaw cycles normalized to average annual number of freeze–thaw cycles (right). Similar plots were produced for the stations at

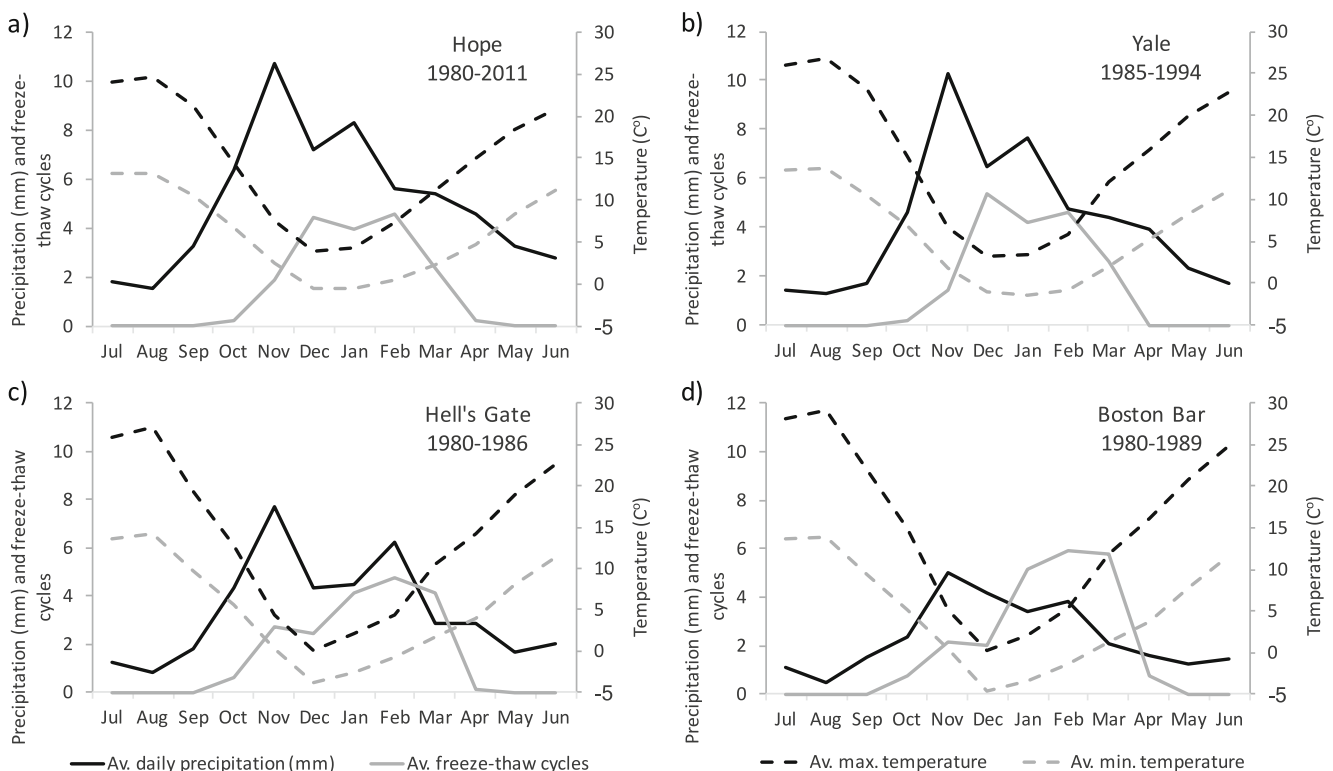


Fig. 5 Seasonal average weather normals (maximum and minimum temperatures, precipitation, and number of freeze–thaw cycles) at Hope (a), Yale (b), Hell's Gate (c), and Boston Bar (d)

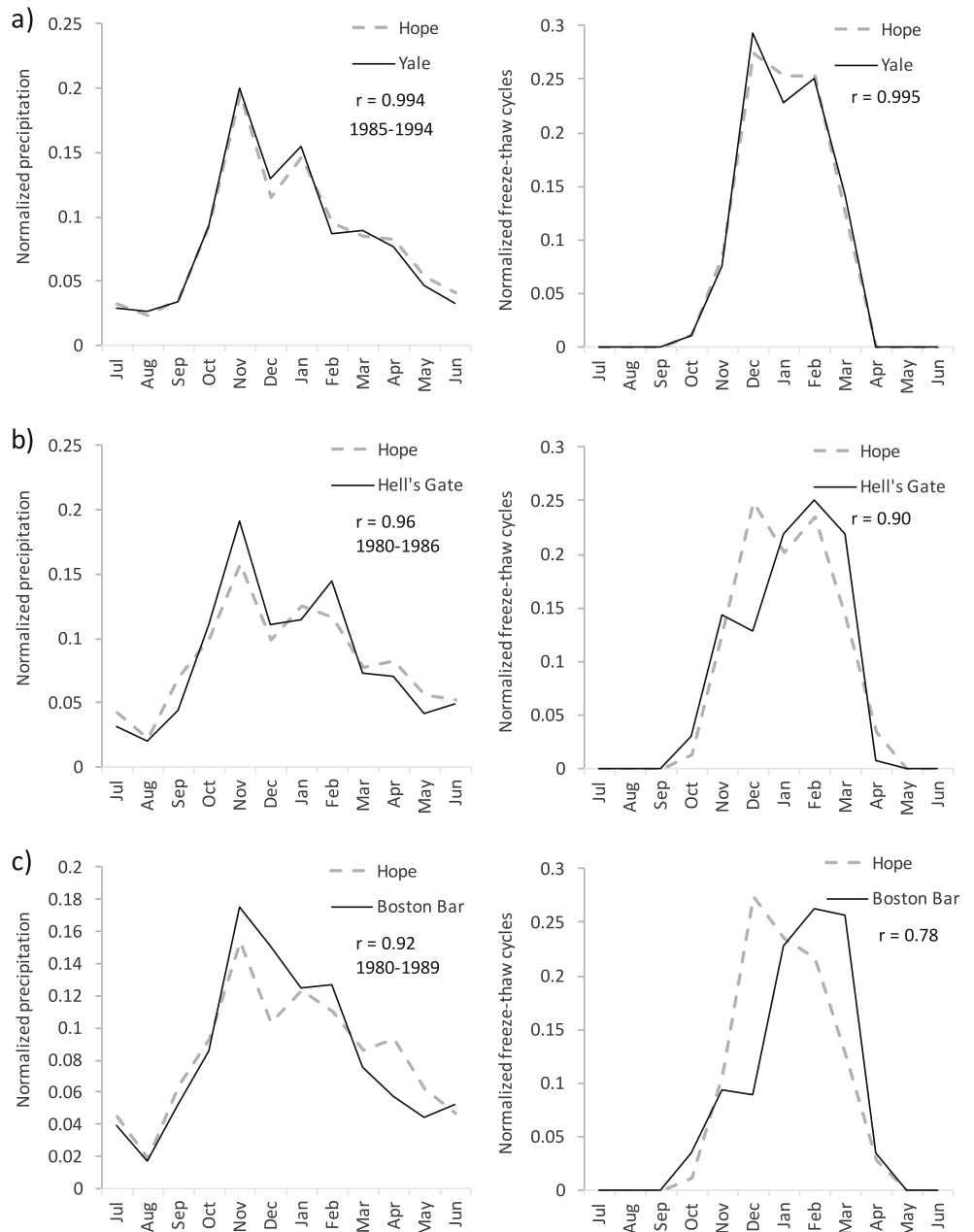
Table 2 Average annual precipitation and freeze–thaw cycles at the four weather stations along the study area

Station	Milepost	Precipitation (mm/year)	Freeze–thaw cycles (no./year)
Boston Bar	3.5	850	22.4
Hell’s Gate	8.5	1211	18.9
Yale	27	1540	18.4
Hope	40	1847	17.7

Yale, Hell’s Gate, and Boston Bar for comparison to those for Hope for the periods for which data were available at Hope and the weather station being evaluated.

The correlation coefficient (*r*) was adopted to evaluate the level of correlation between weather data at Hope and the other stations. It measures the degree to which two

Fig. 6 Correlation of normalized precipitation and freeze–thaw cycles between Hope and Yale (a), Hell’s Gate (b), and Boston Bar (c)



variables change linearly with each other, and is estimated using (Baecher and Christian 2003):

$$r = \frac{E[(x-\mu_x)(y-\mu_y)]}{\sqrt{E[(x-\mu_x)^2] E[(y-\mu_y)^2]}} \tag{1}$$

where r is the correlation coefficient for variables X and Y , $E[\]$ is the expectation operator (defined as the sum of possible values of a random variable weighted by its probability), and μ_x and μ_y are the means of variables X and Y , respectively.

The correlation coefficients for monthly precipitation are shown in Fig. 6 and ranged from 0.92 at Boston Bar to 0.994 at Yale. This level of correlation is considered relatively strong and acceptable for the purposes of this report. Freeze–thaw cycles have weaker correlations due to the temporal shift of cycles at the more northerly stations, with values of 0.78 at Boston Bar, 0.90 at Hell’s Gate, and 0.995 at Yale (Fig. 6). Overall, the correlations between Hope and the other stations are considered acceptable and, therefore, justify using Hope’s weather trends to evaluate rock fall trends north of Hope in terms of seasonal fluctuations.

Finally, Fig. 7 shows the monthly distribution of precipitation and freeze–thaw cycles at Hope and the monthly distribution of rock falls between mileposts 4 and 15 for the period from 1998 and 2011. Rock falls in Fig. 7 are presented as expected annual frequency, calculated as the total number of rock falls in the month divided by the number of years in record. The expected frequency between April and September is low, between 0.1 and 0.6 (a rock fall every 2 to 10 years). These frequencies increase in October (one rock fall annually), with a peak in January (four rock falls annually). Precipitation increases sharply in September to a November peak and follows a downward trend to May. Freeze–thaw cycles begin to increase in November towards high frequencies through December, January, and February.

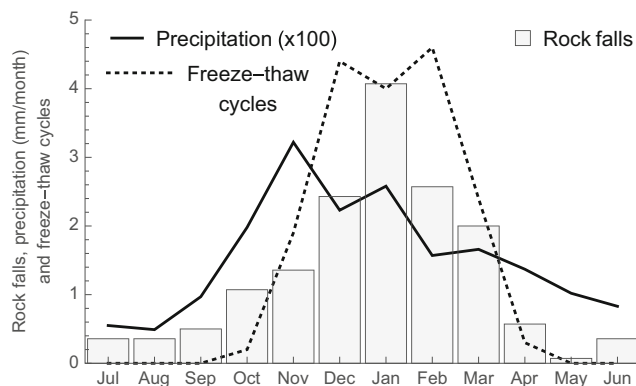


Fig. 7 Precipitation and freeze–thaw cycles at Hope and monthly distribution of annual rock fall frequency between mileposts 4 and 15

Circular distribution fit to weather trend data

Macciotta et al. (2015b) report that precipitation and freeze–thaw cycles are the two main triggers of rock falls along a portion of CN’s Squamish subdivision near Lillooet, BC. Furthermore, a study along a section of railway located along the west bank of the Fraser River Valley reports close correlations between rock fall frequency and precipitation, freeze–thaw cycles, and spring melt (Macciotta et al. 2013). Therefore, the study presented here focuses on quantifying the relationship between rock fall occurrences and monthly trends in precipitation and freeze–thaw cycles.

von Mises circular distributions

Circular distributions are generally used in applications where directional data are being analyzed; however, they are also commonly used to represent cyclic time series data (Bentley 2006; Lark et al. 2014). The circular approach considers data to be distributed continuously on a circle, rather than separating the period into a discrete range within a line of real numbers (Macciotta et al. 2017b). It is still useful, however, to visualize circular distributions on a straight line, keeping in mind that the boundaries are continuous (the probability density function is equal at both ends of the linear visualization).

The von Mises probability density function is one type of circular distribution considered to be a particularly strong tool for statistical inference in modeling circular data problems (Mardia 1972). The von Mises probability density function is defined as follows:

$$M(\mu_0, \kappa) = \frac{1}{2\pi I_0(\kappa)} e^{\kappa \cos(\omega - \mu_0)}, \quad 0 < \omega \leq 2\pi \quad \kappa > 0 \quad 0 \leq \mu_0 < 2\pi \tag{2}$$

where $M(\mu_0, \kappa)$ is the von Mises probability density function, ω is the variable (transformed to equivalent angle), μ_0 is the mean direction (angle), κ is a concentration parameter (a measure of how close the data are to the mean), and $I_0(\kappa)$ is the modified Bessel function of the first kind and order zero:

$$I_0(\kappa) = \sum_{r=0}^{\infty} \frac{1}{r!^2} \left(\frac{1}{2} \kappa\right)^{2r} \tag{3}$$

The seasonality of rock fall triggers (in particular with respect to precipitation and freeze–thaw cycles) can be fitted to von Mises distributions.

Transformation to circular data

Prior to fitting average monthly data, records must be transformed into angular data. In the particular case of monthly

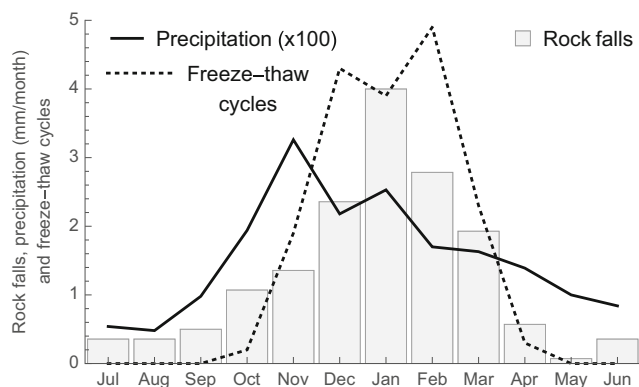


Fig. 8 Adjusted values of average monthly precipitation, number of freeze–thaw cycles (Hope station), and annual rock fall frequency (mileposts 4 to 15)

data, each month can be assigned a range of $\pi/6$. However, because months are not equal in length (number of days), the recorded frequencies require some adjustment, as follows:

- Multiply the recorded frequency of the months with 31 days by the ratio 30/31.
- Multiply the recorded frequency for the month of February by the ratio 30/28. Note that this simplifies the approach for leap years; however, the ratios would only vary by 0.9% when considering leap years (28.25 days on average for the month of February). This does not represent a significant variation in the number of adjusted rock falls for the month of February.
- To maintain the total number of records as per the original, multiply the previously adjusted frequencies by the ratio S/S' , where S is the original total number of records and S' is the sum of records obtained after the first two steps.

Adjusted values of average monthly precipitation, number of freeze–thaw cycles, and expected rock falls (unadjusted values in Fig. 7) are presented in Fig. 8. Table 3 compares the recorded and adjusted values of average monthly precipitation at Hope, average number of freeze–thaw cycles, and total number of rock falls between 1998 and 2011 from mileposts 4 to 15.

Normalization and compatibility scaling

Distribution fitting required data normalization into relative frequencies. This was performed by dividing the average monthly value of precipitation, freeze–thaw cycles, and rock falls by the average annual totals:

$$\text{Normalized value for month } i = \frac{\text{value for month } i}{\sum \text{monthly values}} \quad (4)$$

Distribution fitting also required scaling the weather and rock fall data with a range of 12 months to the von Mises distributions with an angular range of 2π . For this, data arrangement prior to fitting the circular distributions to the adjusted, normalized data must consider the relative position of each month with respect to the angular range of the distribution (2π). For this study, data are arranged starting in July, such that observed distribution peaks in precipitation and freeze–thaw cycles in the winter months are fully displayed. Values of monthly precipitation, freeze–thaw cycles, and rock fall records are plotted at the mid-month location. Given that each month is allocated an equivalent angular range in the circle of $\pi/6$, the values for the month of July (precipitation, freeze–thaw cycles, and rock falls) are plotted at $\pi/12$. The following months are plotted at $\pi/6$

Table 3 Recorded and adjusted values of average monthly precipitation at Hope, average number of freeze–thaw cycles, and total number of rock falls between 1998 and 2011 from mileposts 4 to 15. Total rock falls are calculated as the expected frequency in Figs. 7 and 8 multiplied by the number of years in the record (14 years)

Month	Average precipitation (mm)		No. of freeze–thaw cycles per month		Total no. of rock falls 1998–2011	
	Recorded	Adjusted	Recorded	Adjusted	Recorded	Adjusted
July	55	54	0	0	5	5
August	49	48	0	0	5	5
September	97	98	0	0	7	7
October	198	194	0.2	0.2	15	15
November	322	326	1.9	1.9	19	19
December	223	218	4.4	4.3	34	33
January	258	253	4	3.9	57	56
February	157	170	4.6	4.9	36	39
March	166	163	2.4	2.3	28	27
April	137	139	0.3	0.3	8	8
May	102	100	0	0	1	1
June	83	84	0	0	5	5

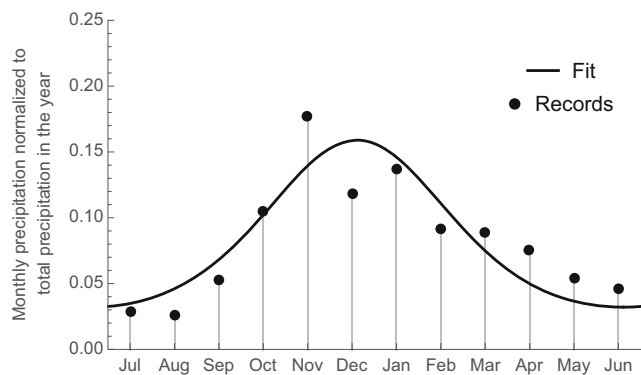


Fig. 9 von Mises distribution fit to normalized monthly precipitation at Hope

intervals, with August plotted at $\pi/12 + \pi/6$, September at $\pi/12 + \pi/3$, and so on.

Further, the von Mises distribution has a total range of 2π and direct comparison to data relative frequencies over 12 monthly values requires scaling the von Mises estimated frequencies. This was achieved by multiplying the von Mises probability density function by a scaling factor of $\pi/6$:

$$\text{Probability Density Function (von Mises)} \times (\pi/6) \quad (5)$$

The frequencies thus obtained from Eq. (5) for the von Mises distributions at the mid-month locations ($\pi/12$ and at increments of $\pi/6$ thereafter) can be directly compared with the adjusted and normalized records. Moreover, the scaled distribution yields a cumulative value of one (1) when evaluated over 12 months.

Precipitation and freeze–thaw cycles fitted to von Mises distributions

Figure 9 shows the monthly precipitation at Hope between 1998 and 2011 (Fig. 8 and Table 3) normalized to the average annual precipitation. This figure also shows a von Mises distribution fitted to the adjusted precipitation data.

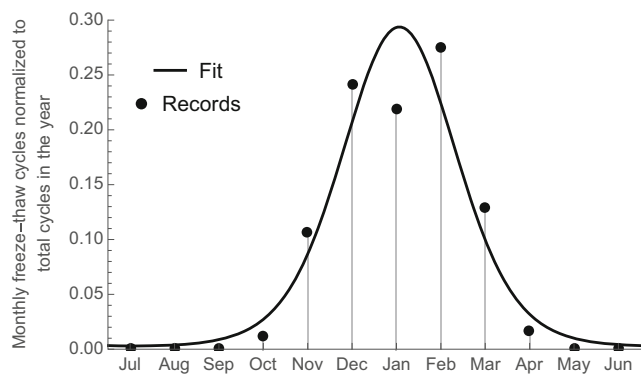


Fig. 10 von Mises distribution fit to normalized freeze–thaw cycles at Hope

Table 4 Summary of von Mises parameters and correlation coefficients for the rock fall triggers

von Mises	μ_0	κ	Correlation coefficient (r)
Precipitation	2.7 (mid-December)	0.8	0.88
Freeze–thaw cycles	3.2 (mid-January)	2.3	0.95

The parameters of the von Mises distribution for the fit are $\mu_0 = 2.7$ (mid-December) and $\kappa = 0.8$. The correlation coefficient for this fit is 0.88. Distribution fitting was done manually to maximize the correlation coefficient.

Figure 10 shows the monthly number of freeze–thaw cycles at Hope between 1998 and 2011 (Fig. 8 and Table 3) normalized to the average annual number of cycles. This figure also shows a von Mises distribution fitted to the adjusted data. The parameters of the von Mises distribution for the fit are $\mu_0 = 3.2$ (mid-January) and $\kappa = 2.3$. The correlation coefficient for this fit is 0.95.

Table 4 summarizes the von Mises parameters and correlation coefficients. The authors considered these correlations strong for the purposes of representing the seasonality of rock fall triggers.

Rock fall distribution model

Aggregation of the von Mises distribution fits of precipitation and freeze–thaw cycles into a model of the seasonal distribution of rock falls can be achieved through a weighted sum or mixture distribution (Macciotta et al. 2017b):

$$F_M = \sum_{j=1}^m W_j F_j(\omega) \quad (6)$$

where F_M is the mixture distribution, $F_j(\omega)$ is the j th von Mises cumulative distribution, and W_j is the relative weight for the j th distribution. The condition for the weights is that their sum is equal to 1 ($\sum W_j = 1$).

The weighted mixture distribution was fitted to the rock fall distributions through calibration of the distribution weights to maximize the correlation coefficient. Table 5 shows the calibrated weights for each von Mises distribution. Figure 11 shows the rock fall trigger von Mises distributions, monthly rock fall relative frequencies, and the mixture distribution fitting the rock fall data. The correlation coefficient between the mixture distribution and rock fall records is 0.97.

Table 5 Calibrated weights for the rock fall trigger von Mises distributions

von Mises	W_j
Precipitation	0.3
Freeze–thaw cycles	0.7

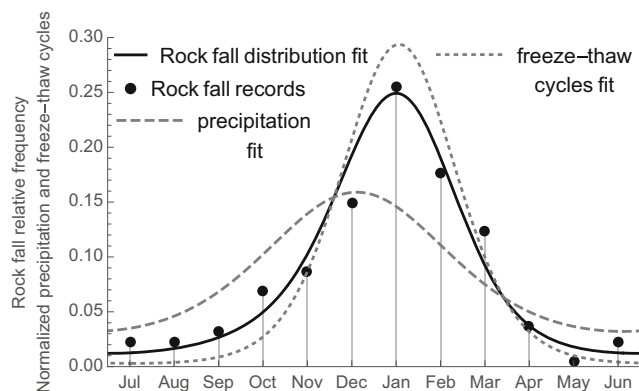


Fig. 11 Precipitation and freeze–thaw cycles fit distributions, weighted distribution fit to rock fall records, and rock fall relative frequency

Conclusions

This paper presented a case study for the application of a methodology that allows quantification of the relationship between the seasonality of weather and rock fall occurrences. The method is based on modeling rock fall weather triggers' cyclic annual trends by fitting circular probability distributions and modeling rock fall annual trends through aggregation of the fitted weather models.

The methodology was first proposed by Macciotta et al. (2017b) for a section of a transportation corridor through the Canadian Cordillera. The work presented here illustrates the applicability of the methodology to other locations of the Cordillera. Moreover, this work suggests some standardized procedures for data management, including transformation of records to circular data, setting the month of July as the initiation point for the circular distribution, and scaling the von Mises distributions to match the 12-month range of the cyclic period. These standardized procedures will allow future direct comparison of the outcomes of this approach among different locations.

In the case study presented here, rock fall trends correspond to a slope cut on intrusive rock along a section of a transportation corridor that was 17.7 km long. Average annual precipitation and number of freeze–thaw cycles in the area are 850 mm and 22.4, respectively. Precipitation and freeze–thaw cycles were fitted to von Mises distributions with correlation coefficients of 0.88 and 0.95, respectively, and combined with weights of 30 and 70%, respectively. The resulting model had a correlation coefficient of 0.97 with respect to rock fall records. The weights used in the mixture distribution (70% for the freeze–thaw and 30% for the precipitation annual trends) suggest that the temporal occurrence of rock fall events peaks is dominated by freeze–thaw cycles as the trigger mechanism along this section of study. On the contrary, Macciotta et al. (2017b) found that precipitation had a larger influence on rock fall annual distribution along a different area in the Canadian Cordillera (weight of up to 81%). This was expected as the

area of analysis in their study was closer to the sea and milder temperatures resulted in less freeze–thaw cycles per year.

It was mentioned in the introduction that, for the region where the study area is located, precipitation is projected to decrease in the summer and fall and the timing for freeze–thaw cycles to concentrate on the winter months and decrease during the fall and spring. Given the influences of precipitation and freeze–thaw cycles suggested by the results of this study, rock fall occurrences would be expected to decrease in the summer and fall and to further be concentrated in the winter months.

Although the methodology allows direct and quantitative correlation between weather patterns and rock fall trends, the findings and insights are limited to general rock fall trends within a year and their expected shift with changes in weather patterns. It was mentioned that other studies have shown the potential influence of increased intensity of weather events and localized storms in landslide occurrences (Coe 2017; Ho et al. 2017; Delonca et al. 2014; Raveland and Deline 2011, 2015; Paranunzio et al. 2015, 2016; Macciotta et al. 2015b), and these should complement the insights from studies similar to the one presented here on rock fall pattern changes. Limitations and room for improvement also include the following:

- Quantitative relationships consider relative frequencies within a year without regard for weather and rock fall variations from one year to another. This would require extending the approach to other cyclic phenomena (e.g., decadal weather oscillations, El Niño events).
- von Mises distributions are unimodal distributions (one peak only). Some weather triggers can be argued to present bimodal behaviors, reflecting the true nature of the phenomena (e.g., freeze–thaw cycles at the beginning and end of the colder season). This can be addressed by fitting a combination of two or more distributions such that the bimodality is better reflected, but would increase the complexity of the model and its interpretation. Such decisions require understanding of climate patterns on a case-by-case basis and should reflect the purposes of the analysis.
- The method allows analysis of the general trends of rock falls within the year but not short-term estimates of rock fall probabilities based on weather events. In this regard, the method provides a means of forward modeling rock fall trend changes for changes in climatic trends. Short-term forecasting requires complementary approaches (e.g., Macciotta et al. 2015b).

In particular for the case illustrated here, weather records needed to be validated for a weather station 50 km away from the study area. Although precipitation distributions showed remarkably good correlations, the freeze–thaw cycles

correlation was lower. This presents a challenge for the application of the methodology. In this regard, Hell's Gate station is located within the section of analysis (milepost 7, and the detailed analysis is for mileposts 4 to 15) and freeze–thaw cycles show a general good correlation with Hope, with the exception of December. The inconsistency in the peak for freeze–thaw cycles represents a limitation for the application of the method in this particular section by adding uncertainty in the rock fall correlations. This highlights the importance of consistent weather records in proximity of the study area.

The influence of weather triggers on the distribution of rock falls likely depends on the rock mass characteristics of the rock fall sources. The method presented here focused on a section that shared consistent geologic characteristics. A case study database is being built following the method outlined in this paper for different rock mass characteristics. This will allow for the analysis of weather and rock fall trends common to different triggers or different geologic units. The method provides a means to quantify the effects of climate variations in rock fall trends, and the authors encourage the application of this method to aid in building this case study database and strengthening the tools.

Acknowledgements The authors acknowledge the Canadian National Railway Company (CN) for providing the data that made this study possible. This research was made possible by the (Canadian) Railway Ground Hazard Research Program.

References

- Baecher GB, Christian JT (2003) Reliability and statistics in geotechnical engineering. John Wiley & Sons, Chichester, West Sussex, 605 pp
- Bentley J (2006) Modelling circular data using a mixture of von Mises and uniform distributions. Department of Statistics and Actuarial Science, Simon Fraser University. A project submitted in partial fulfillment of the requirements for the degree of Master of Science
- Bunce CM, Cruden DM, Morgenstern NR (1997) Assessment of the hazard from rock fall on a highway. *Can Geotech J* 34:344–356
- Bush EJ (2015) Plenary 2: climate change in Canada: observations and projected changes. In: Proceedings of Mine Water Solutions in Extreme Environments, Vancouver, Canada, April 2015, pp 6–19
- Bush EJ, Loder JW, James TS, Mortsch LD, Cohen SJ (2014) An overview of Canada's changing climate. In: Warren FJ, Lemmen DS (ed) Canada in a changing climate: sector perspectives on impacts and adaptation. Government of Canada, Ottawa, pp 23–64
- Cloutier C, Locat J, Geerstema M, Jakob M, Schnorbus M (2017) Potential impacts of climate change on landslides occurrence in Canada. In: Ho K, Lacasse S, Picarelli L (eds) Slope safety preparedness for impact of climate change. CRC Press, Taylor & Francis Group, London, pp 71–104
- Coe JA (2017) Landslide hazards and climate change: a perspective from the United States. In: Ho K, Lacasse S, Picarelli L (eds) Slope safety preparedness for impact of climate change. CRC Press, Taylor & Francis Group, London, pp 479–523
- Delonca A, Gunzburger Y, Verdell T (2014) Statistical correlation between meteorological and rockfall databases. *Nat Hazards Earth Syst Sci* 14:1953–1964
- Douglas GR (1980) Magnitude frequency study of rockfall in Co. Antrim, N. Ireland. *Earth Surf Process* 5:123–129
- Environment Canada (2017) Government of Canada, Meteorological Service of Canada. <http://climate.weather.gc.ca>. Accessed June 2017
- Evans SG, Hungr O (1993) The assessment of rockfall hazard at the base of talus slopes. *Can Geotech J* 30:620–636
- Frayssines M, Hantz D (2006) Failure mechanisms and triggering factors in calcareous cliffs of the Subalpine Ranges (French Alps). *Eng Geol* 86:256–270
- Higgins JD, Andrew RD (2012) Rockfall types and causes. In: Turner AK, Schuster RL (ed) Rockfall characterization and control. Transportation Research Board, Washington, DC, pp 21–55
- Ho KKS, Lacasse S, Picarelli L (2017) Preparedness for climate change impact on slope safety. In: Ho K, Lacasse S, Picarelli L (eds) Slope safety preparedness for impact of climate change. CRC Press, Taylor & Francis Group, London, pp 104–146
- Hungr O, Evans SG, Hazzard J (1999) Magnitude and frequency of rock falls and rock slides along the main transportation corridors of southwestern British Columbia. *Can Geotech J* 36:224–238
- Kromer RA, Hutchinson DJ, Lato MJ, Gauthier D, Edwards T (2015) Identifying rock slope failure precursors using LiDAR for transportation corridor hazard management. *Eng Geol* 195(C):93–103
- Lan H, Martin CD, Zhou C, Lim CH (2010) Rockfall hazard analysis using LiDAR and spatial modeling. *Geomorphology* 118:213–223
- Lark RM, Clifford D, Waters CN (2014) Modelling complex geological circular data with the projected normal distribution and mixtures of von Mises distributions. *Solid Earth* 5(2):631–639
- Lato MJ, Diederichs MS, Hutchinson DJ, Harrap R (2012) Evaluating roadside rockmasses for rockfall hazards using LiDAR data: optimizing data collection and processing protocols. *Nat Hazards* 60(3): 831–864
- Logan T, Charron I, Chaumont D, Houle D (2011) Atlas de scénarios climatiques pour la forêt québécoise. Ouranos, Ministère des Ressources Naturelles et de la Faune du Québec (MRNF). Available from: <http://www.ouranos.ca/media/publication>. Accessed 10 June 2018
- Luckman BH (1976) Rockfalls and rockfall inventory data: Some observations from surprise valley, Jasper National Park, Canada. *Earth Surf Process* 1:287–298
- Macciotta R, Hendry MT (2017) Rock falls – a deterministic process with nonlinear behavior? In: De Graff JV, Shakoor A (eds) Proceedings of the 3rd North American Symposium on Landslides, Roanoke, Virginia, June 2017, pp 597–606
- Macciotta R, Martin CD (2013) Role of 3D topography in rock fall trajectories and model sensitivity to input parameters. In: Pyrak-Nolte LJ, Chan A, Dershowitz W, Morris J, Rostami J (eds) Proceedings of the 47th US Rock Mechanics/Geomechanics Symposium, San Francisco, California, June 2013, pp 1–9
- Macciotta R, Cruden DM, Martin CD, Morgenstern NR (2011) Combining geology, morphology and 3D modelling to understand the rock fall distribution along the railways in the Fraser River Valley, between Hope and Boston Bar. In: Eberhardt E, Stead D (eds) Slope Stability 2011: Proceedings of the 2011 International Symposium on Rock Slope Stability in Open Pit Mining and Civil Engineering, Vancouver, Canada, September 2011. Canadian Rock Mechanics Association (CARMA), Vancouver
- Macciotta R, Cruden DM, Martin CD, Morgenstern NR, Petrov M (2013) Spatial and temporal aspects of slope hazards along a railroad corridor in the Canadian Cordillera. In: Dight P (ed) Slope Stability 2013: Proceedings of the 2013 International Symposium on Slope Stability in Open Pit Mining and Civil Engineering, Brisbane, Queensland, Australia, September 2013, pp 1171–1186
- Macciotta R, Martin CD, Cruden DM (2015a) Probabilistic estimation of rockfall height and kinetic energy based on a three-dimensional trajectory model and Monte Carlo simulation. *Landslides* 12(4):757–772

- Macciotta R, Martin CD, Edwards T, Cruden DM, Keegan T (2015b) Quantifying weather conditions for rock fall hazard management. *Georisk* 9(3):171–186
- Macciotta R, Martin CD, Morgenstern NR, Cruden DM (2016) Quantitative risk assessment of slope hazards along a section of railway in the Canadian Cordillera—a methodology considering the uncertainty in the results. *Landslides* 13(1):115–127
- Macciotta R, Martin CD, Cruden DM, Hendry M, Edwards T (2017a) Rock fall hazard control along a section of railway based on quantified risk. *Georisk* 11(3):272–284
- Macciotta R, Hendry M, Cruden DM, Blais-Stevens A, Edwards T (2017b) Quantifying rock fall probabilities and their temporal distribution associated with weather seasonality. *Landslides* 14(6):2025–2039
- Mardia KV (1972) *Statistics of directional data*. Academic Press, London, 357 pp
- McTaggart KC, Thompson RM (1967) Geology of part of the northern Cascades in southern British Columbia. *Can J Earth Sci* 4:1199–1228
- Monger JWH (1970) Hope map-area, west half, British Columbia, paper 69-47. Geological Survey of Canada, Department of Energy, Mines and Resources
- Paranunzio R, Laio F, Nigrelli G, Chiarle M (2015) A method to reveal climatic variables triggering slope failures at high elevation. *Nat Hazards* 76:1039–1061
- Paranunzio R, Laio F, Chiarle M, Nigrelli G, Guzzetti F (2016) Climate anomalies associated with the occurrence of rockfalls at high-elevation in the Italian Alps. *Nat Hazards Earth Syst Sci* 16:2085–2106
- Peckover FL, Kerr JWG (1977) Treatment and maintenance of rock slopes on transportation routes. *Can Geotech J* 14(4):487–507
- Pierson LA, Davis SA, VanVickle R (1990) *Rockfall Hazard Rating System: implementation manual*. FHWA report FHWA-OR-EG-90-01. FHWA, U.S. Department of Transportation
- Piteau DR (1977) Regional slope stability controls and engineering geology of the Fraser Canyon, British Columbia. *Rev Eng Geol* 3:85–111
- Ravelin L, Deline P (2011) Climate influence on rockfalls in high-Alpine steep rockwalls: the north side of the Aiguilles de Chamonix (Mont Blanc massif) since the end of the ‘Little Ice Age’. *Holocene* 21(2):357–365
- Ravelin L, Deline P (2015) Rockfall hazard in the Mont Blanc massif increased by the current atmospheric warming. In: Lollino G, Manconi A, Clague J, Shan W, Chiarle M (eds) *Engineering geology for society and territory*, vol 1. Climate change and engineering geology. Springer International Publishing, Cham, Switzerland, pp 425–428
- Rodriguez JL, Macciotta R, Hendry M, Edwards T, Evans T (2017) Slope hazards and risk engineering in the Canadian railway network through the Cordillera. In: DellAcqua G, Wegman F (eds) *Proceedings of the AIT International Congress on Transport Infrastructure and Systems (TIS 2017)*, Rome, Italy, April 2017, pp 163–168
- van Veen M, Hutchinson DJ, Kromer R, Lato M, Edwards T (2017) Effects of sampling interval on the frequency–magnitude relationship of rockfalls detected from terrestrial laser scanning using semi-automated methods. *Landslides* 14(5):1579–1592
- Wieczorek GF, Jäger S (1996) Triggering mechanisms and depositional rates of postglacial slope-movement processes in the Yosemite Valley, California. *Geomorphology* 15:17–31
- Yavuz H (2010) Effect of freeze–thaw and thermal shock weathering on the physical and mechanical properties of an andesite stone. *Bull Eng Geol Environ* 70(2):187–192